Journal of Statistical Physics, Vol. 21, No. 3, 1979

Metastable Chaos: The Transition to Sustained Chaotic Behavior in the Lorenz Model

James A. Yorke[1] and Ellen D. Yorke[2]

Received March 21, 1978; revised March 19, 1979

The system of equations introduced by Lorenz to model turbulent convective flow is studied here for Rayleigh numbers r somewhat smaller than the critical value required for sustained chaotic behavior. In this regime the system is found to exhibit transient chaotic behavior. Some statistical properties of this transient chaos are examined numerically. A mean decay time from chaos to steady flow is found and its dependence upon r is studied both numerically and (very close to the critical r) analytically.

KEY WORDS: Turbulence; chaos; Lorenz system.

1. INTRODUCTION

Chaotic time-dependent behavior is of interest in all sciences and has been most studied in connection with fluid turbulence. In an investigation of an idealized model for the instability of convection of a fluid between two parallel plates, Lorenz introduced a system of ordinary differential equations which, for appropriate parameter values, exhibits "deterministic nonperiodic flow." The solutions, though completely determined by initial conditions, vary with time in a seemingly irregular way. Furthermore, small changes in initial conditions produce large differences in the long-term behavior of the solutions. Thus, to an observer of the gross properties, the system appears to behave in a chaotic fashion.

This work was supported in part by NASA grant NSG 5209; partial support of computer costs was provided by the University of Maryland—Baltimore County Computer Center.

[1] Institute for Physical Science and Technology and Department of Mathematics, University of Maryland, College Park, Maryland.

[2] Department of Physics, University of Maryland—Baltimore County, Catonsville, Maryland.

0022-4715/79/0900-0263$03.00/0

The equations introduced by Lorenz[10] are

$$dx/dt = \sigma y - \sigma x, \qquad dy/dt = -xz + rx - y, \qquad dz/dt = xy - bz \quad (1.1)$$

(See also Marsden and McCracken[12] and Marsden.[13]) While later calculations[3,14] show that they may not be adequate to describe the instability of convective flow in the geometry for which they were devised, they may describe spiking in lasers[3] and they may adequately describe a different convective fluid system, which we shall describe in Section 2. Furthermore, they form a relatively simple model system in which a wealth of irregular behavior may be studied.

This paper presents detailed numerical studies of the Lorenz system in a "preturbulent" parameter range. We restrict ourselves to $\sigma = 10$ and $b = 8/3$ as did Lorenz. For $r < 1$, Lorenz showed solution (0, 0, 0), representing no convection, is stable, while for $r > 1$ there are three critical points: (0, 0, 0), $(\alpha, \alpha, r - 1)$, and $(-\alpha, -\alpha, r - 1)$, where $\alpha = [b(r - 1)]^{1/2}$. For r between 1 and r_2 [where $r_2 = \sigma(\sigma + b + 3)(\sigma - b - 1)^{-1}$, which is approximately 24.74 for the above choice of parameters] the two nonzero solutions are stable and attracting, and for $r > r_2$, all three critical points are unstable.[4] Lorenz observed sustained chaotic oscillations for $r = 28$ and he described in detail the trajectories in phase space and the strange attracting set in which they lie.[5] This strange attractor is observed to be completely dominant for r in the range just above $r_2 \approx 24.74$ and in particular for the case $r = 28$ studied by Lorenz. Almost any initial condition (x_0, y_0, z_0) yields a trajectory that approaches the strange attractor. It can actually be observed for values of r slightly below r_2. In a range $r_1 \approx 24.06 < r < r_2$ some trajectories tend to the strange attractor asymptotically, while others tend asymptotically to the stable attracting points. The former trajectories are observed to oscillate irregularly without ever settling down. Small changes in initial data are observed to result in large differences in the long-term pattern of oscillations. Hence we may say that for $r > r_1$ we observe "sustained chaos." (For much larger $r > 50$ the behavior begins to change and we ignore this range.)

[3] Haken[6] shows that an equivalent system can be derived for lasers, but it is not clear to us that the laser parameter corresponding to σ is large enough for the system to oscillate chaotically.

[4] At r_2 the system has an "inverted bifurcation." That is, since the rest point p becomes unstable as r increases past r_2, no stable point or periodic orbit is seen near p. However, an inverted bifurcation is not necessary for the type of behavior we discuss in this paper. In particular, Marsden and McCracken[12] have found that for small σ the Hopf bifurcation for the Lorenz system is regular.

[5] A strange attractor may be thought of as an attracting invariant set that looks strange, that is, it is a bounded, connected set which is neither a point nor a periodic orbit nor a surface. The term was coined by Ruelle and Takens,[16] but was not defined precisely.

The purpose of this paper is to describe the transition at r_1 and in particular to describe the dynamics for r just below r_1.

It is shown by Kaplan and Yorke[7,8] that at $r = r_0 \approx 13.926$ a transition occurs (see also Robbins[16,17] for a discussion of this preturbulent regime). Immediately above r_0 there is an "exceptional" set (i.e., measure zero, very small) of chaotic orbits which oscillate forever. The chaotic set exists but is unstable for r between r_0 and r_1: it is dynamically like a saddle, so that most initial conditions chosen close to, but not on, the set will yield trajectories which eventually diverge from the set. If an initial condition (x, y, z) is chosen at random from a neighborhood of this small chaotic set, the probability is zero that it oscillates forever without damping out. Though this oscillatory (or chaotic) set is thus not directly observable, its existence affects what is observed in our numerical investigations, especially for r just below r_1. The "decay time" for orbits near the chaotic set is surprisingly long for

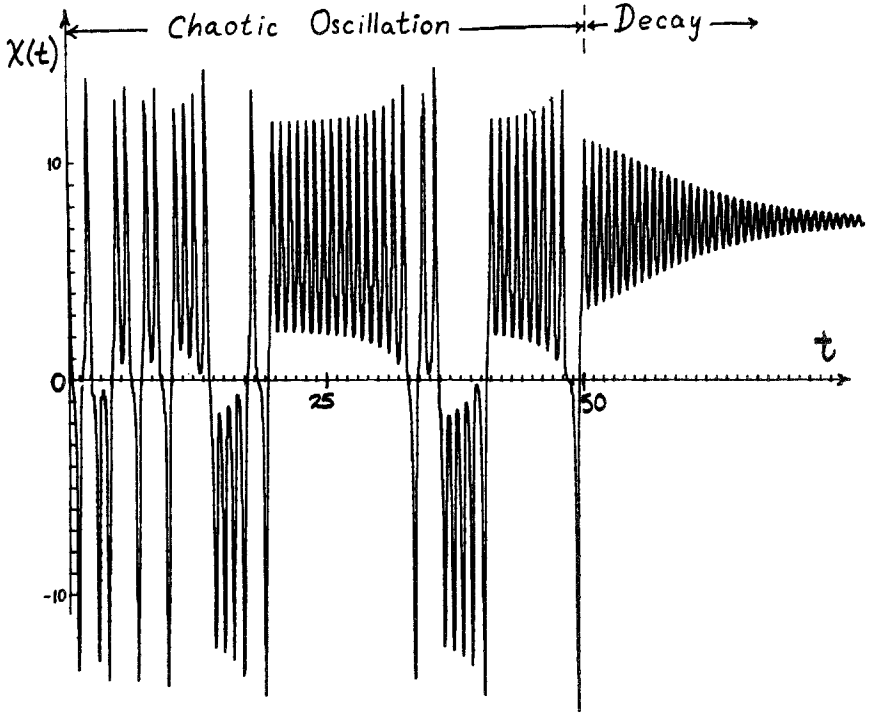

Fig. 1. This solution of (1.1) using $r = 22$ exhibits a transient chaotic behavior which suddenly switches to a pattern of oscillation that decays to the equilibrium $x = \pm[(r - 1)(8/3)]^{1/2}$. On the average, chaotic behavior switches to damped behavior after about 60 oscillations. For larger $r < r_1 \simeq 24.06$, chaotic behavior persists longer, over 300 oscillations on the average for $r = 23.0$.

r just below r_1 and it is this "metastable" feature that we emphasize in this paper. Figure 1 illustrates the type of behavior we are discussing, in particular a sudden transition from irregular to damped oscillation.

2. REPRESENTATION OF SYSTEM VIA A SCALAR FUNCTION

Lorenz showed that there is an ellipsoid E in R^3 such that every trajectory would eventually cross into the ellipsoid and, once inside, would remain inside. That is, the ellipsoid is positively invariant under the differential equations. Write $\phi(p, t) \in R^3$ for the position in R^3 of the solution of Eq. (1.1) at time t, starting from $p \in R^3$. For a set $S \subset R^3$ write $\phi(S, t)$ for $\{\phi(p, t): p \in S\}$. Denote the three-dimensional volume of S by $\mathrm{Vol}(S)$. Lorenz observed that the divergence of the right-hand side of Eq. (1.1) is constant, $-(\sigma + b + 1)$. Hence,

$$\mathrm{Vol}(\phi(S, t)) = \exp[-t(\sigma + b + 1)] \cdot \mathrm{Vol}(S) \tag{2.1}$$

Let E be the positively invariant ellipsoid mentioned above. Since $\phi(E, t) \subset E$ for t positive, it follows that

$$\phi(E, t_1) \subset \phi(E, t_2) \qquad \text{if} \quad t_1 > t_2 > 0$$

Every trajectory tends asymptotically to the limiting set,

$$E_\infty = \bigcap_{t>0} \phi(E, t)$$

as t tends to infinity, and it follows from (2.1) that this set has volume zero. The shape of E_∞ is extremely complex for $r > r_0 \simeq 13.9$. For $r > r_0$, E_∞ contains some trajectories which oscillate forever, aperiodically, without ever settling down to constant or periodic behavior. For $r \simeq r_1 \simeq 24.06$, the average time per oscillation observed in numerical experiments [i.e., the average time between successive maxima of a particular coordinate, say $z(t)$] may be taken as approximately 2/3. Considering this a characteristic time of the system, the corresponding volume contraction factor is $\exp[-(2/3)(10 + 8/3 + 1)] \approx 0.00013$. Hence any initial point in the general region of interest yields a trajectory which rapidly approaches the set E_∞, possibly tending asymptotically to some point or subset of E_∞, possibly eventually winding arbitrarily close to every point of a "strange" set E_∞.

We numerically integrated the Lorenz system. Our differential equation solver was a divided difference form of Adams–PECE local extrapolation, adapted from a program of Shampine.

For $r > r_1$ it is easy to find trajectories which appear to oscillate irregularly, as long as they are followed numerically. This is indeed the behavior we would expect from theoretical investigations. On the other hand, for

r slightly less than r_1 similar irregular oscillations are observed, persisting for many cycles, but eventually they begin to damp down to one of the two stable equilibria $x = y = \pm[b(r-1)]^{1/2}$, $z = r - 1$. In particular, numerical studies show the $x(t)$ coordinate changes sign occasionally throughout the irregular oscillations, but $x(t)$ finally achieves a constant sign as the solutions tend to one of the equilibria. We define the final time T at which x changes sign to be the beginning of the decay and the end of the irregular period (see Fig. 1). If no sign change exists, we let $T = 0$. For an initial point $P = (x_0, y_0, z_0)$, we count the number of local maxima of the z coordinate of the trajectory during the irregular period $(0, T)$. We call this the oscillation number $N(P)$ of the point P.

An apparent dichotomy appears for r slightly less than r_1. For many initial points, $N(P) = 0$ or 1, and these are points whose trajectories begin to decay almost immediately. For example, points near the stable critical points yield $N(P) = 0$ and points near the unstable critical point (0, 0, 0) yield $N(P) = 1$. The other type of point P yields a large $N(P)$. For $r = 23.0$, for example, in trial runs the average value of $N(P)$ is about 300, considering only points for which $N(P) > 1$.

This apparent dichotomy is difficult to analyze by direct numerical integration of (1.1) because the average $N(P)$ appears to tend to infinity rapidly as $r \to r_1 \approx 24.06$ and excessive computer time is required, even at $r = 23$. Also, the trajectories are quite unstable; small changes in initial conditions produce large differences in oscillation pattern after the first several oscillations. Inevitable numerical errors result in uncertainties in the position and these uncertainties seem to double approximately on each oscillation until the error dominates the situation. Hence our calculations of $N(P)$ are suggestive, but are not accurate. Also, simple computations of averages of $N(P)$ do not yield an intuitive understanding of the transition at $r = r_1$.

Lorenz described a surprising technique for reducing the complexity of Eq. (1.1) from an ordinary differential equation in R^3 to a function of one variable. Solving the systems of equations numerically, he recorded the successive peaks of the coordinate $z(t)$ (this choice of z is somewhat arbitrary.) Denoting the nth maximum of $z(t)$ by M_n, he plotted successive pairs (M_n, M_{n+1}) of maxima and found they lay along a sharply peaked, Λ-shaped curve. He reported that "within the limits of the round-off in tabulating z" he found a precise two-to-one relation between M_n and M_{n+1}. That is, the graph appeared to describe a function $M_{n+1} = \Lambda(M_n) = \Lambda(r, M_n)$. This relation does not hold exactly (even for the exact solutions), but deviations are quite small. If a second trajectory is chosen for the same r and its successive maxima $\tilde{M}_n$ are calculated, the successive pairs $(\tilde{M}_n, \tilde{M}_{n+1})$ will lie along the same graph (except possibly for the first or second pair). When taking a long sequence of local maxima, the pairs seem to fill out the graph of

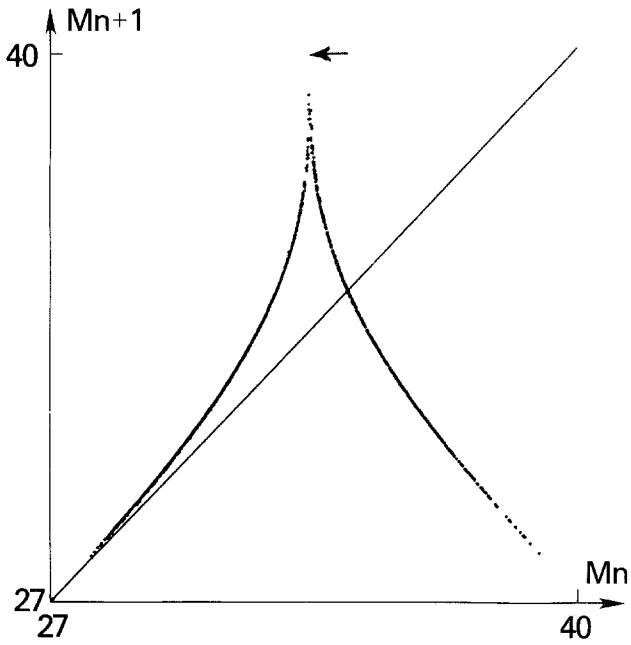

Fig. 2a. A solution of (1.1) with $r = 24.06$ was computed numerically and the first 2000 peaks (denoted M_n, with $n = 1,..., 2000$) of $z(t)$ were tabulated. The diagonal is drawn for comparison. The closer the trajectory comes to (0, 0, 0), the higher the next peak value will be, and the arrow indicates the largest possible value of M_{n+1}, a value which results from an extremely close approach to (0, 0, 0). The system (1.1) has a periodic orbit with a peak z value of approximately 26.9. Almost every chaotic trajectory will give peak values of z that trace out the same figure. Compare with Fig. 3.

Λ quite well. See Li and Yorke[9] for a discussion of the possible behaviors of $\{\Lambda(M_n)\}$ when $r = 28$; see also Sharkovskii.[19]

For $r < r_1$ we cannot generate the entire graph using a single trajectory since beyond some time, the trajectory tends asymptotically to a constant so that the pairs (M_n, M_{n+1}) tend asymptotically to $(r - 1, r - 1)$. To describe the graph of $\Lambda(r, M_n)$ in detail we have chosen numerous initial points and then chosen 35–45 such pairs of maxima. Figure 2 shows a typical case, $r = 22.0$. We exclude the first few maxima from consideration. These maxima are usually chosen from the irregular oscillation part of the curve. We then fitted a curve to the data using $\lambda(r, M)$ of the form

$$\lambda(M) = Z_{\max} - A_1|M - M_0|^{\beta}(1 + A_2|M - M_0| + A_3|M - M_0|^2) \quad (2.2)$$

where A_1, A_2, A_3, β, and M_0 are to be determined using the least squares technique. As can be seen in the figures of Lorenz, the largest values observed for z are the local maxima that follow close approaches of the trajectory to

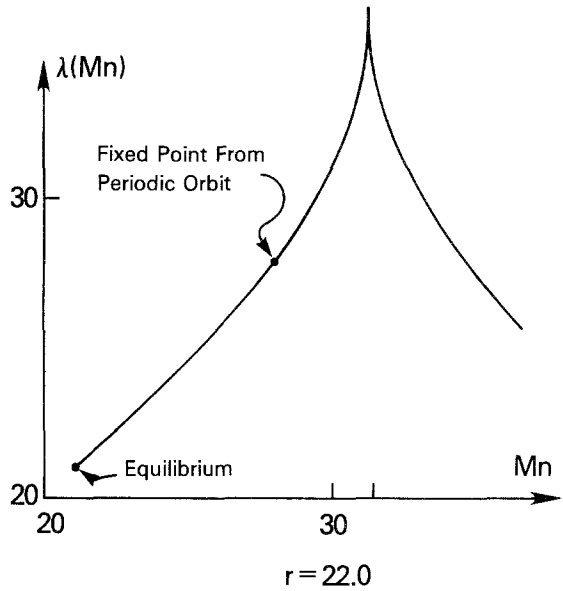

Fig. 2b. The pattern of data (M_n, M_{n+1}) in Fig. 2a can be approximated by a curve, though this pattern has a small nonzero width. An approximating curve is shown for $r = 22.0$. Once a trajectory has a peak z value less than the peak for the periodic orbit (approximately 28.0 for $r = 22.0$) the sequence of peaks M_n decays monotonically as the oscillation damps down to equilibrium. To obtain a curve as given here a number of trajectories must be used together since for $r = 22$, on the average about 60 values of M_n are obtained before decay sets in. In this paper we are primarily interested in fitting the part of the curve to the right of the fixed point, since we wish to analyze the statistics of when decay sets in.

(0, 0, 0). Consequently, the value $Z_{\max}$ is chosen to be the first maximum when starting from a point quite near (0, 0, 0). In order to estimate the nature of the peak, several of the pairs were chosen with second coordinate quite large. Also, there is a trajectory which is periodic with $x(t)$ of constant sign. The successive maxima of this orbit are constant. We obtained initial points that gave an accurate approximation to this periodic trajectory in order to determine the local maxima M_{per} of the z coordinate of this trajectory, and we chose the unknown parameters A_1, A_2, A_3, β, and M_0 so that

$$\lambda(M_{\text{per}}) = M_{\text{per}}$$

since this point plays a special role. When a maximum M_n is found such that $M_n < M_{\text{per}}$ the trajectory is in the process of decaying to a constant. By contrast, the periodic orbit yielding M_{per} by definition does not decay. The parameters were chosen for the r values 21.0, 22.0, 23.0, 23.5, and 24.0.

Table I

r	$Z_{\max}$	M_0	M_{per}	β
24	40.724	33.795	27.002	0.285
23.5	39.771	33.199	27.551	0.295
23	38.819	32.602	27.839	0.299
22	36.916	31.405	27.977	0.302
21	35.016	30.210	27.765	0.310

Tables I and II summarize the results of this procedure. On the average, 34 points were used to fit the data for each value of r. A root-mean-squared deviation of less than 0.01 was obtained for each value of r.

It is surprising that such a good fit as we obtained was achievable using the function λ, which is assumed to be symmetric. We have no explanation for the symmetry in the data.

The calculated coefficients Z_m and M_0 are almost linear functions of r. The exponent β is quite difficult to determine accurately. The fit is relatively insensitive to small changes in β. The shape of λ near the peak depends on trajectories that pass near (0, 0, 0), since, as mentioned earlier, the largest values of M_n occur after trajectories pass close to (0, 0, 0). The linearized system at (0, 0, 0) has three eigenvectors with eigenvalues $\lambda_b = -b$ and $\lambda_\pm = (-\sigma - 1 \pm \rho)/2$, where $\rho = [(\sigma + 1)^2 - 4\sigma(1 - r)]^{1/2}$. In our range of investigation we have $\lambda_- < \lambda_b < 0 < \lambda_+$. Trajectories approaching (0, 0, 0) do so generically along the eigenvector corresponding to λ_b. Those moving away from (0, 0, 0) do so along the eigenvector corresponding to λ_+. Heuristic arguments can be given that the actual β should be the ratio $|\lambda_b/\lambda_+|$. Such a trajectory will lie nearly in the plane having eigenvalues λ_b and λ_+ as long as it is near (0, 0, 0). Hence it will temporarily nearly satisfy a linear planar differential equation

$$y_1' = \lambda_b y_1, \qquad y_2' = \lambda_+ y_2$$

where coordinates are chosen so that (0, 1) and (1, 0) correspond to eigen-

Table II

r	A_1	A_2	A_3
24	5.936	0.0571	−0.00106
23.5	5.779	0.0527	−0.00092
23	5.591	0.0528	−0.00084
22	5.165	0.0631	−0.00202
21	4.788	0.665	−0.00240

vectors. Solutions of this system satisfy $y_1(t)^{\lambda_+} y_2(t)^{|\lambda_b|} = \text{const}$, so a trajectory that passes near (0, 0) will approach through some point $(\epsilon, 1)$ (for ϵ small but nonzero) and will depart through a point $(\pm 1, \psi(\epsilon))$, where $\psi(\epsilon) = |\epsilon|^{|\lambda_+/\lambda_b|}$. Recall that trajectories through $(\pm 1, 0)$ correspond to the trajectory that has a peak value $z_{\max}$ and the corresponding solution of the nonlinear system can be expected to have a peak which is smaller than $z_{\max}$ by an amount proportional to $\psi(\epsilon)$.

At $r = 24.0$, $|\lambda_b/\lambda_+| = 0.251+$, as opposed to the table value of 0.2850. Hence the theoretical value would yield an even sharper peak in λ than the one we found. The discrepancy may be due to the insensitivity of λ to β and the fact that relatively large errors in β correspond to much smaller errors in the (M_n, M_{n+1}) pairs.

3. LONG-TERM STATISTICAL BEHAVIOR

The functions $\lambda(M)$ in Section 2 give us a tool for investigating the nature of the temporary chaotic behavior illustrated in Fig. 1 for some r values. Iterating these functions allows us to circumvent the prohibitive expense of numerically integrating the differential equations through a large number of cases, involving altogether about a million oscillations of the system. We examine sequences

$$M_{n+1} = \lambda(M_n) \tag{3.1}$$

In this section we report findings in terms of the normalization

$$u = \tfrac{1}{2}(M - M_{\text{per}})/(M_0 - M_{\text{per}})$$

Corresponding to a sequence $\{M_n\}$ we have a corresponding sequence $\{u_n\}$ which lies in [0, 1] as long as it oscillates irregularly. We also write $u_{n+1} = \lambda(u_n)$ or $\lambda(r, u_n)$. In this notation λ is symmetric about $u = 1/2$ and the peak value $\lambda(1/2) > 1$, while $\lambda(0) = 0 = \lambda(1)$. We define the *peak width* $w = w(r)$ to be the size of the interval (with center $u = 1/2$) on which $\lambda(u) > 1$; that is,

$$\lambda(r, 1/2 - w/2) = 1 = \lambda(r, 1/2 + w/2)$$

(see Figure 2). The critical value r_1 is the first value for which λ maps [0, 1] into [0, 1] and hence $\lambda(r_1, 1/2) = 1$.

For each of three values of r we broke [0, 1] into N_r subintervals of equal size. In each subinterval an initial point was chosen using a pseudo-random number generator with a uniform probability distribution. For each of these initial values u_0, we iterate λ, examining $u_n = \lambda(r, u_{n-1})$, $n = 1, 2, \ldots$, (calculated in double precision) until a value $u_n^{\S}$ is obtained with $u_n > 1$ or until $n = 2000$, whichever is smaller, and write $n(u_0)$ for this resulting integer. Hence for each of N_r values of u_0, a kickout time $n(u_0)$ was obtained. The average value of $n(u_0)$ is what we report as the average decay time $\langle n \rangle$.

Table III

r	Initial points, N_r	Mean, $\langle n \rangle$	Kickout probability, $\langle n \rangle^{-1}$	Peak width at $\lambda = 1$
21	20,000	22.0	0.045	0.041
22	20,000	59.6	0.017	0.014
23	4,000	312.4	0.0032	0.0023

Our results are summarized in Table III. N_r is smaller for larger r values because of the larger number of iterations required. At the end of this section we present a method for estimating how the average decay time depends on r for r slightly below r_1, where any technique would be expensive. For each $r = 21$, 22, and 23, we calculated the frequency distributions. $\phi(n)$ is the number of initial points out of the N_r chosen that had kickout times equal to n.

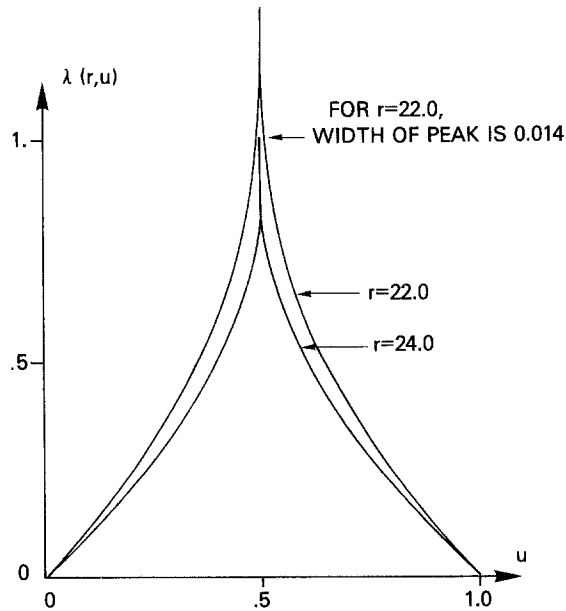

Fig. 3. After rescaling so that λ is defined on [0, 1], the peak value of the curve, namely $\lambda(r, 1/2)$, exceeds 1 (provided $r < r_1 \simeq 24.06$). The "width of the peak" is the size of the interval of u values for which $\lambda(r, u) > 1$. This width is found to be roughly proportional to the reciprocal of the average number of chaotic oscillations of a solution prior to the onset of decay.

(See Fig. 3.) We hypothesized that this distribution would be the same as if the kickout times were exponentially distributed. A simple nonrigorous way to test this is to calculate the number of points whose kickout time exceeded n and to plot the logarithm against n. The points should—and did—lie nearly on a straight line. We tested further and more precisely the hypothesis that there is a probability $p(r)$ of kickout per iteration which is independent of n. Choosing $p(r)$ to be the reciprocal of average kickout time, the expected value of $\phi(n)$ would be $N_r p(r)[1 - p(r)]^n$. We aggregated the data and used a χ^2 test to determine whether the deviations of the observed $\phi(n)$ from the expected values were reasonably small. The χ^2 test demonstrated that all were acceptable at the 90% probability level.

If points are distributed in [0, 1] with some initial probability density f_0, then the images $\lambda(u_0)$ that remain in [0, 1] will have some (in general, other) probability density we may denote f_1. In our case u_0 was uniformly distributed so that $f_0 \equiv 1$. We may similarly write f_n for the density of nth iterate images $\lambda^n(u_0)$ that remain in [0, 1]; f_n is normalized so that $\int_0^1 f_n = 1$. If $(1/2 - w/2, 1/2 + w/2)$ denotes the interval where $\lambda(u) > 1$, then $\Pi_n = \int_{1/2-w/2}^{1/2+w/2} f_n$ is the probability that $\lambda^n(u_0)$ will be in the peak width interval, given that it is in [0, 1]. Hence Π_n is the probability that a point which has survived n iterations will be kicked out on the $(n + 1)$th iteration. Exponential decay will be observed if Π_n tends rapidly to some constant $\Pi^* > 0$. We define $1/\Pi^*$ to be the *mean kickout time*. Pianigiani and Yorke[15] have proved that f_n converges to a "smooth" (infinitely differentiable) limiting density f^* and this limit is independent of the initial density f_0, as long as f_0 is continuous and strictly positive. While Pianigiani and Yorke deal with more general cases, they show the conclusion is valid if λ satisfies the following properties:

1. λ: $[0, 1] \to R$.

2. There are numbers $0 = a_0 < a_1 < \cdots < a_k = 1$ such that λ is infinitely differentiable on each (a_{i-1}, a_i) and $(0, 1) \subset \lambda((a_{i-1}, a_i))$ for $i = 1, \ldots, k$.

3. There are $L_1 > L_2 > 0$ such that $L_1 \geqslant |d\lambda(x)/dx| \geqslant L_2$ whenever $\lambda(x) \in (0, 1)$.

For our situation $a_1 = 1/2$ and $a_2 = 1$. The hypotheses are also satisfied by a map which appears quite different, namely $\lambda(x) = rx(1 - x)$ provided $r > 2 = 5^{1/2}$. The limit f^* depends on λ and so depends on r. Hence

$$\Pi^*(r) = \lim \Pi_n = \int_{1/2-w/2}^{1/2-w/2} f^* > 0$$

When the initial distribution is the uniform distribution (i.e., $f_0 \equiv 1$), we observe a rapid relaxation, $f_n \to f^*$ in the sense that $\int |f_n - f^*|$ decreases by a factor of approximately 0.9 per iteration up to $n = 20$. Although these

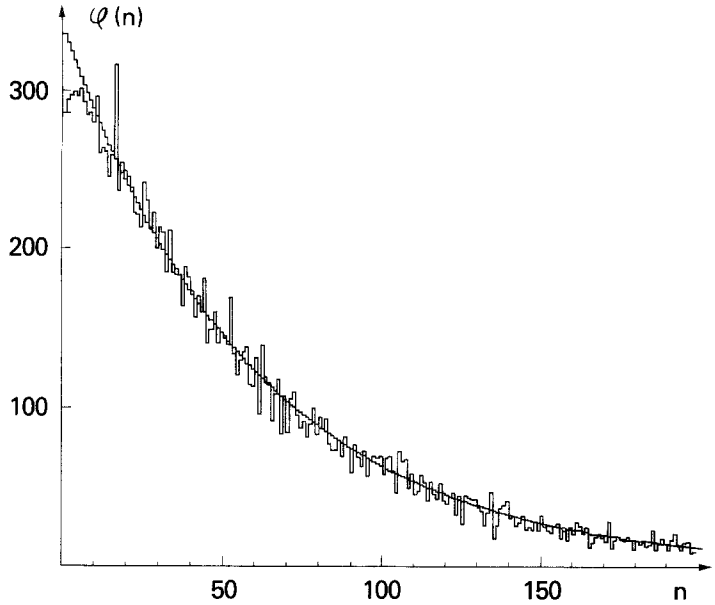

Fig. 4. Frequency distribution of kickout time n for $r = 22.0$. The exponential $(N_r/\mu)\exp(-n/\mu)$, where $N_r = 20{,}000$ and $\mu = 59.6$, is plotted for comparison.

observations are crude, they do indicate that the relaxation of $\int |f_n - f^*|$ to zero is rapid in comparison with the kickout time. Figure 4 shows a small initial deviation from a good exponential decay for n up to 5 or 10. We attribute this to the relaxation of the shape of f_n to f^*.

In describing the transition at $r = r_1$ it is useful to have an analytical expression giving the approximate dependence of the average kickout time upon r for r close to r_1. From Eq. (3.1) we see that the reciprocal of the kickout time depends upon both the peak width and the limiting distribution f^* in the interval of the peak. We can rewrite Eq. (4.1)

$$\Pi^*(r) = \langle f^*(r)\rangle w(r)$$

where $\langle f^*(r)\rangle$ is the average of f^* over the peak width. If we assume that $\langle f^*(r)\rangle$ tends to a finite, nonzero constant as $r \to r_1$, then for r sufficiently close to r_1

$$\Pi^*(r) \approx \langle f^*(r_1)\rangle w(r)$$

and the chief dependence of the kickout time upon r will be due to the decrease of the peak width to zero as r tends to r_1.

The peak width can be estimated from the equation for the curve $\lambda(r, u)$. We have been dealing specifically with the normalized form of Eq. (2.2)

$$\lambda = \lambda_{\max} - |u - 1/2|^{\beta}(A_1' + A_1'A_2'|u - 1/2| + A_1'A_3'|u - 1/2|^2)$$

where $\lambda_{\max}$, β, and the coefficients A_i' are functions of r. If we let $x = |u - \frac{1}{2}|$ we have a particular equation of the approximate form

$$\lambda(x, r) = \lambda_{\max}(r) - x^{\beta}[A_1'(r) + o_x(1)] \tag{3.2}$$

where $o_x(1)$ denotes a function which tends to zero as $x \to 0$. In general $o_x(\cdots)$ denotes terms of higher order than whatever is inside the parentheses. The following argument will depend only upon the behavior of λ near the peak and so will hold for functions other than the explicit form used in Section 2. We now write $A(r)$ for $A_1'(r)$. Assume λ has the form in Eq. (3.2), where $A(r_1) > 0$. For $r < r_1$, $\lambda_{\max} > 1$ and for $r = r_1$, $\lambda_{\max} = 1$, and we assume $(d/dr)\lambda_{\max}(r) \neq 0$ at r_1. Write

$$f_r(x) = x[A(r) + o(1)]^{1/\beta}$$

Notice $(d/dx)f_r(0) = A(r_1)^{1/\beta}$, so f_r has an inverse for x near zero.

To solve for the width w, i.e.,

$$\lambda(r, w/2) = 1, \qquad r \leqslant r_1$$

we write Eq. (3.2) as $1 = \lambda_{\max}(r) - f_r(w/2)^{\beta}$. Hence

$$\begin{aligned} f_r(w/2) &= [\lambda_{\max}(r) - 1]^{1/\beta} \\ w/2 &= f_r^{-1}([\lambda_{\max}(r) - 1]^{1/\beta}) \\ &= \frac{1}{f_r'(0)}\{[\lambda_{\max}(r) - 1]^{1/\beta} + o_{r_1 - r}([\lambda_{\max}(r) - 1]^{1/\beta})\} \\ &= A(r_1)^{-1/\beta}\left[\frac{d}{dr}\lambda_{\max}(r_1)(r - r_1)\right]^{1/\beta}[1 + o_{r_1 - r}(1)] \end{aligned}$$

as $r \to r_1$. Hence the kickout time is approximately equal to $\alpha(r_1 - r)^{-1/\beta}$, where α is a constant. For notational simplicity we have treated β as a constant, but the argument is easily adapted to allow β to depend on r, provided $\beta(r_1) \neq 0$, and the conclusion is unchanged.

This approximation will hold only for r sufficiently close to r_1. For the range of values covered in Table III, the validity of the approximation is exceeded.

4. DISCUSSION

In the preceding work we have discussed the metastable chaotic behavior of the Lorenz model with Rayleigh number r somewhat below the critical value r_2 at which an inverted bifurcation occurs. At these lower values the system exhibits metastable chaos as shown in Fig. 1. After a large number of irregular oscillations, the system damps down to one of its two stable states.

The "lifetime" in the chaotic states depends on initial values and is distributed exponentially. We have examined this behavior numerically and have presented an analytic estimate of the decay time for r just below r_1. This decay time tends rapidly to infinity as $r \to r_1 \approx 24.06$. For $r \geqslant r_1$ sustained chaotic oscillations can be observed. The decay time is proportional to $(r_1 - r)^{-1/\beta}$, where $1/\beta$ is between 3.5 and 4 for our choice of σ and b. The metastable chaotic behavior for $r < r_1$ is a precursor of the situation for $r > r_1$, in which there are two coexisting types of regimes, a chaotic regime and a steady state (laminar) regime. For $r < r_1$ our metastable chaos might be thought of as a leaky chaos in which trajectories can pass through a small "window" in the chaotic region and on into the stationary region.

For historical reasons we have chosen the "canonical" Lorenz model parameters, which seem to be widely used in the literature of numerical studies of the Lorenz equations.[11]

In general one might seek out metastable states by varying parameters in physical systems where steady-state and chaotic regimes coexist. The chaotic regime may cease to exist, as some controlling parameter is varied, by changing into a metastable chaotic regime. Creveling *et al.*[2] decreased the Rayleigh number past a critical value (our r_1). They passed from an unstable to a stable flow situation, yet they observed irregular oscillations which persisted sometimes as long as 2 h (corresponding to 100–200 oscillations). This is the sort of behavior which would be expected if metastable chaos is occurring. Although the boundary conditions used in that experiment were such that the Lorenz equations do not describe the system, there is no reason to expect that metastable chaos is peculiar to the Lorenz model or even to systems in which an inverted bifurcation occurs. We suggest that Creveling and his co-workers might have observed metastable chaos.

In what other types of systems might metastable chaos occur? Suitable systems are those in which at least two stable states coexist, one of which shows regular, easily describable time dependence (steady state or periodic) while another one is turbulent. Such will be the case if the system has a finite-amplitude instability so that a perturbation of minimum size is needed to knock the system from one regime to the other. The existence of a finite-amplitude instability guarantees the existence of at least two regimes. Similarly, systems with hysteresis have the property that at least two regimes coexist, since the state that is observed depends on the history of the system. In particular, pipe flow and channel flow exhibit laminar states which can be knocked into turbulent regimes by small though finite perturbations. And in his study of Couette flow between cylinders rotating in opposite directions Coles[1] has observed situation where turbulent and laminar regimes coexist. In these situations metastable chaos might be observed as the system is brought from a stable turbulent regime to a stable steady state. (As one can see in this

paper, it might, in practice, be difficult to measure precisely the critical parameters for a turbulent-to-steady-state transition, since it is possible to have metastable chaos with such a long lifetime that it is virtually indistinguishable from sustained chaos.)

ACKNOWLEDGMENTS

We thank R. F. Chang for providing us with his curve fitting program, which he developed in the investigation of the critical exponents for phase transition of binary fluids, and R. Kaylor for his help in programming. We thank A. Faller for discussions and for introducing us to Lorenz's papers in 1968.

REFERENCES

1. D. Coles, *J. Fluid Mech.* **21**:385 (1965).
2. H. F. Creveling, J. F. dePaz, J. Y. Baladi, and R. J. Schoenhals, *J. Fluid Mech.* **67**:65 (1975).
3. J. Curry, A Generalized Lorenz System Having Invariant Tori, Preprint (1977).
4. V. S. Eframovich, V. V. Bikov, and L. P. Silnikov, *Dokl. Akad. Nauk SSSR* **234**:336 (1977).
5. J. Guckenheimer, Structural Stability of the Lorenz Attractors, Preprint (1978).
6. H. Haken, *Phys. Lett.* **53A**:77 (1975).
7. J. L. Kaplan and J. A. Yorke, Preturbulence: A Regime Observed in a Fluid Flow Model of Lorenz, *Comm. Math. Phys.*, in press.
8. J. L. Kaplan and J. A. Yorke, The Onset of Chaos in a Fluid Flow Model of Lorenz, in *Proceedings of New York Acad. Sci. Meeting on Bifurcation* (1977).
9. T. Y. Li and J. A. Yorke, *Am. Math. Monthly* **82**:985 (1975).
10. E. N. Lorenz, *J. Atmos. Sci.* **20**:130 (1963).
11. M. Lucke, *J. Stat. Phys.* **15**, 455 (1976).
12. J. E. Marsden and M. McCracken, *The Hopf Bifurcation and its Applications* (Springer-Verlag, New York, 1976).
13. J. E. Marsden, in *Turbulence Seminar* (Springer-Verlag Lecture Notes in Math., No. 615, 1977).
14. J. B. McLaughlin and P. C. Martin, *Phys. Rev. A* **12**:186 (1975).
15. G. Pianigiani and J. A. Yorke, *Trans. Am. Math. Soc.*, in press.
16. K. A. Robbins, *Proc. Nat. Acad. Sci.* **73**(12):4296 (1976).
17. K. A. Robbins, *Math. Proc. Camb. Phil. Soc.*, to appear (1977).
18. D. Ruelle and F. Takens, *Comm. Math. Phys.* **20**:167 (1971); **23**:343 (1971).
19. A. N. Sharkovskii, Coexistence of the Cycles of a Continuous Mapping of the Line into Itself (in Russian), *Ukr. Math. J.* **16**(1):61 (1964).
20. P. Welander, *J. Fluid Mech.* **29**:17 (1967).
21. W. V. R. Malkus, *Mem. Roy. Sci. Liège, Ser. 6* **4**:125 (1972).
22. R. F. Williams, The Structure of Lorenz Attractors, *Publ. Inst. Hautes Etudes Sci.*, in press; see also R. F. Williams and J. Guckenheimer, Structural Stability of Lorenz Attractors, *ibid.*